

Permanent Electrochemical Doping of Quantum Dots and Semiconductor Polymers

Gudjonsdottir, Solrun; Houtepen, Arjan J.

DOI

[10.1002/adfm.202004789](https://doi.org/10.1002/adfm.202004789)

Publication date

2020

Document Version

Final published version

Published in

Advanced Functional Materials

Citation (APA)

Gudjonsdottir, S., & Houtepen, A. J. (2020). Permanent Electrochemical Doping of Quantum Dots and Semiconductor Polymers. *Advanced Functional Materials*, 30(49), Article 2004789. <https://doi.org/10.1002/adfm.202004789>

Important note

To cite this publication, please use the final published version (if applicable). Please check the document version above.

Copyright

Other than for strictly personal use, it is not permitted to download, forward or distribute the text or part of it, without the consent of the author(s) and/or copyright holder(s), unless the work is under an open content license such as Creative Commons.

Takedown policy

Please contact us and provide details if you believe this document breaches copyrights. We will remove access to the work immediately and investigate your claim.

Permanent Electrochemical Doping of Quantum Dots and Semiconductor Polymers

Solrun Gudjonsdottir and Arjan J. Houtepen*

Arguably the most controllable way to control the charge density in various semiconductors, is by electrochemical doping. However, electrochemically injected charges usually disappear within minutes to hours, which is why this technique is not yet used to make semiconductor devices. In this manuscript, electrochemical doping of different semiconductor films (ZnO Quantum Dots (QDs), PbS QDs, and P3DT) is investigated in various high melting-point nitrile-based solvents. It is shown that by charging the semiconductors at elevated temperatures, then cooling down to room temperature where these solvents are frozen, the doping stability increases immensely. Measurements performed in cyanoacetamide show that ion transport is entirely halted at room temperature, and that the n-type conductivity is stable for days, and only drops marginally ($\approx 10\%$) in several weeks. For p-doped P3DT films, the conductivity is even completely stable during the entire 76 days of the measurement. In an ambient atmosphere, the p-type doping is stable, while the n-type doping disappears in several hours, as electrons react with molecular oxygen. Finally, a pn-junction diode made of a PbS QD film is demonstrated. These results highlight the possibility of using solidified electrolytes for electrochemical doping and for obtaining semiconductor devices wherein the doping density is controlled electrochemically.

1. Introduction

Over the last decades, various promising semiconductor materials have emerged, including colloidal quantum dots (QDs) and organic semiconductors. These semiconductors are known for their facile and cheap solution synthesis and their tunable optoelectronic properties.^[1,2] Therefore, they are promising for, and indeed already used in, various semiconductor devices such as LEDs, light emitting electrochemical cells (LECs), lasers and solar cells.^[2d,3] In order to use semiconductors in various devices, control over the charge carrier density is critical. There

are, in principle, various ways to dope the abovementioned semiconductors, e.g. via impurity doping,^[4] or photodoping,^[5] although these methods are often faced with difficulties in controlling the charge density and the stability of the charge density.^[6,7]

Arguably, the most controllable way of doping films of semiconductor QDs or organic semiconductors is via electrochemical doping. In this approach a semiconductor film is deposited on the working electrode (WE), and a potential is applied versus the reference electrode (RE) in an electrochemical cell. By changing the potential of the WE toward more negative potentials, electrons can be injected into the conduction band of the material (Figure 1a). In contrast, by applying more positive potentials, electrons can be extracted from the valence band. Therefore, the desired charge carrier density can be obtained by controlling the applied potential.^[8] Essential for efficient electrochemical doping is that counterions are able to permeate the semiconductor films to provide charge neutrality. For films of QDs, fullerenes and organic semiconductors this is typically the case, so that electrochemical doping is a practical and generic method for all of them.

Unfortunately, it is usually observed that the injected charge density is not stable: when the electrochemical cell is disconnected from the potentiostat the semiconductor film discharges spontaneously, as is depicted in Figure 1b.^[8a,9] The main reasons for this self-discharge are intrinsic electrochemical reactions and redox reactions with impurities, typically oxygen or water.^[10] Thus, in order to stabilize the doping density, the diffusion of the electrolyte ions and impurities should be minimized.

Electrochemically injected charges can be stabilized by freezing the electrolyte solvent (Figure 1c,d). Guyot-Sionnest et al. and Houtepen et al. showed stable electrochemically doped semiconductor films at cryogenic temperatures.^[11] These films were stable for days, but as soon as the temperature was increased the injected charge left the films. The same trend was observed by Heeger et al. for light emitting electrochemical cells (LECs), where the LECs were only stable at 200 K or lower.^[3f,12] Clearly, it is not suitable to keep the films at cryogenic temperatures if they are to be used as semiconductor devices. Lately, extensive research has been going on to stabilize LECs at room temperature. While these measures increased the doping stability, unfortunately, none of them produced stable LECs at room temperature.^[13]

Electrochemically injected charges can be stabilized by freezing the electrolyte solvent (Figure 1c,d). Guyot-Sionnest et al. and Houtepen et al. showed stable electrochemically doped semiconductor films at cryogenic temperatures.^[11] These films were stable for days, but as soon as the temperature was increased the injected charge left the films. The same trend was observed by Heeger et al. for light emitting electrochemical cells (LECs), where the LECs were only stable at 200 K or lower.^[3f,12] Clearly, it is not suitable to keep the films at cryogenic temperatures if they are to be used as semiconductor devices. Lately, extensive research has been going on to stabilize LECs at room temperature. While these measures increased the doping stability, unfortunately, none of them produced stable LECs at room temperature.^[13]

S. Gudjonsdottir, Prof. A. J. Houtepen
Chemical Engineering
Optoelectronic Materials
Delft University of Technology
Van der Maasweg 9, Delft 2629 HZ, The Netherlands
E-mail: A.J.Houtepen@tudelft.nl

 The ORCID identification number(s) for the author(s) of this article can be found under <https://doi.org/10.1002/adfm.202004789>.

© 2020 The Authors. Published by Wiley-VCH GmbH. This is an open access article under the terms of the Creative Commons Attribution License, which permits use, distribution and reproduction in any medium, provided the original work is properly cited.

DOI: 10.1002/adfm.202004789

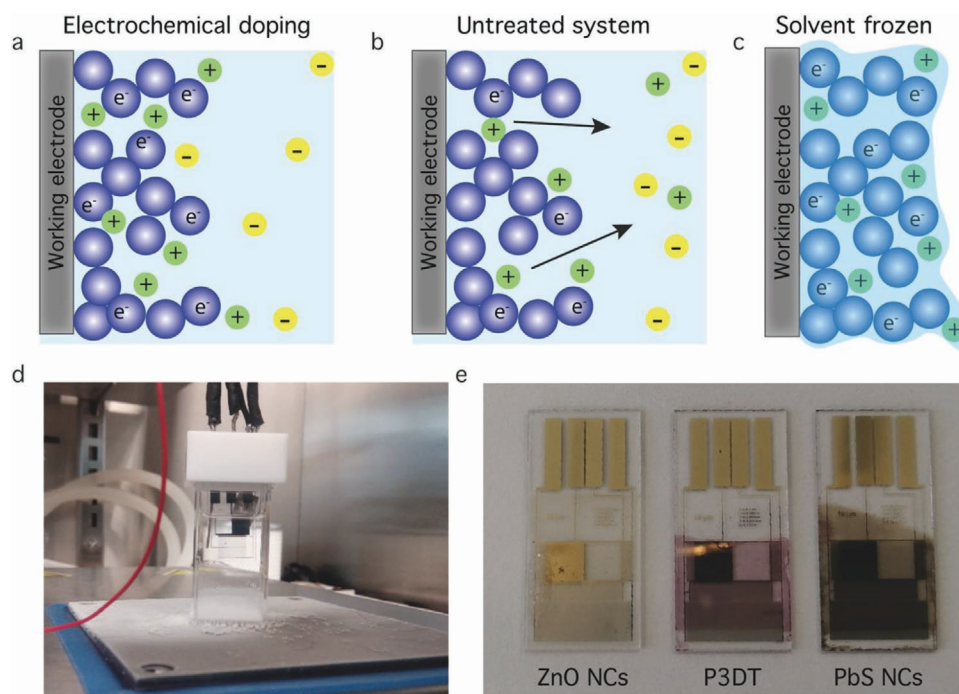


Figure 1. Electrochemical doping of semiconductor films by freezing the electrolyte solvent. a) When a negative enough potential is applied to the working electrode, electron injection takes place. Electrolyte cations diffuse into the voids of the film to neutralize the injected charge. b) When a doped semiconductor film is disconnected from the potentiostat, injected charges disappear. c) By freezing the electrolyte solvent before the potentiostat is disconnected, the doping stability is retained. d) Electrochemical measurement performed at low temperature on a hot/cold plate. e) Semiconductor films used in this study: ZnO NCs, P3DT, and PbS NCs.

In a previous study, we investigated electrolyte solvents with melting points above room temperature.^[10b] Various semiconductor films were charged at elevated temperature where the electrolyte solvent was liquid, and their doping stability was measured at lower temperatures. Surprisingly, the solvent with the highest melting point (mp), dimethyl sulfone (mp: 109 °C), did not show the best stability at room temperature. A probable explanation for this is that other factors than the melting point play a role. For example the impurity concentration, the electrochemical stability of the solvent and how well it can crystallize at room temperature inside and on top of a semiconductor film.

Although the room temperature stability was increased greatly in our previous study, no solvent showed a truly stable electrochemically doped film at room temperature. However, by using succinonitrile (mp: 57 °C) as the electrolyte solvent, a fully stable electrochemically doped ZnO QD film was achieved at -75 °C. This suggests that a high melting point reduction occurs inside the semiconductor films, and only at -75 °C electrolyte ions and impurities have become immobile. It appears that succinonitrile is a suitable solvent for electrochemical doping, with low impurities content and high intrinsic electrochemical stability, however its melting point is too low for stable doping at room temperature. Taking inspiration from these results we have searched for chemically similar nitrile solvents with higher melting points.

In most cases the melting point of a molecule can be increased by increasing the molecular weight, adding aromaticity (to enhance the crystallinity in the solid state) or hydrogen bond forming groups such as alcohols.^[14] In this paper we investigate three different semiconductor films (ZnO NCs, PbS NCs, and P3DT, Figure 1e) and four different nitriles

with high melting points: trans-3-hexenedinitrile (mp: 76 °C), cyanoacetamide (mp: 120 °C), 1,2-dicyanobenzene (mp: 138 °C) and 1,3-dicyanobenzene (mp: 164 °C). We start by determining the electrochemical stability window of the solvents. Thereafter, we perform electrochemical doping and stability measurements on ZnO QD films. All solvents except trans-3-hexenedinitrile, show no charge injection at room temperature, which means that ion diffusion essentially does not happen. At temperatures above the mp, all solvents can be used to charge the ZnO QD films with electrons. When cooling down after charging, the n-doping of the films is retained. However, we observe a clear correlation between the stability of the electron density and the cathodic stability limit of the solvent. This shows that reduction of the solvent is an important factor in the charge stability of electrochemically doped films. Additionally, if the melting point of the solvent is not high enough, as is the case for trans-3-hexenedinitrile, the electron density gradually decreases. Of the solvents used, the stability of the doping density at RT was best for cyanoacetamide, in line with its superior cathodic stability. Therefore this solvent was chosen for a more in-depth analysis of the RT doping stability in ZnO QD films.

From an electrochemical analysis it is determined that at 140 °C, when cyanoacetamide is liquid, the diffusion coefficient of the Li⁺ ions is found to be $\approx 10^{-9}$ cm² s⁻¹, while it drops to $\approx 10^{-21}$ cm² s⁻¹ at RT. This means that it would take a cation more than 300 000 years to diffuse through the 1 μm thick ZnO QD film. Clearly, from an ion diffusion perspective the doping should be stable. Long-term conductivity measurements on doped ZnO QD films show that the electron density is fully stable over 20 hours. On much longer time scales there is a

slow but noticeable decrease in the conductivity; after 10 days, 80% of the initial conductivity is retained, if the sample is stored in an inert atmosphere glovebox.

Given the very low diffusion coefficient of the ions, the observed drop in conductivity is likely caused by electrochemically active impurities (most likely oxygen). As solid cyanoacetamide is amorphous, it is possible for oxygen to penetrate the cyanoacetamide layer and react with injected electrons in the ZnO QD film. Indeed, taking a doped ZnO QD film out of the glovebox and exposing it to air causes the conductivity to drop to almost zero in about two hours. However, by placing a blocking layer such as PMMA on the film, the doping stability in air is increased greatly. This method does not only work for ZnO QDs but also for PbS QD films and P3DT films (poly(3-decylthiophene-2,5-diyl)). For n-doped PbS QD films, the RT conductivity is entirely stable for over 5 days. However, as for the ZnO QD film the electrons gradually leave the film and after 40 days almost 10% of the injected charge has left the film. Interestingly, for p-doped P3DT films the conductivity decays only by 2% over the span of over 76 days. Additionally, when the film is taken out of the glovebox, the conductivity is not affected at all. This is most likely because oxygen is the main impurity responsible for the instability of n-doped films, whereas the stability of p-doped films is not affected by oxygen, but typically by water. Finally, this approach was used to form a pn-junction diode constructed of PbS QDs. This shows the promise for electrochemically doped semiconductor films.

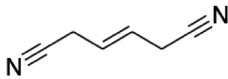
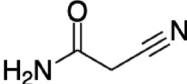
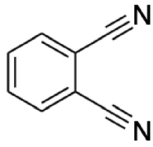
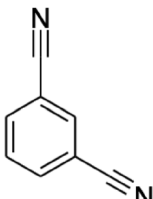
2. Results and Discussion

Our previous results showed that succinonitrile, despite a melting point of the pure solvent of 57 °C, was not fully crystallized at

RT when used as an electrolyte solvent to dope ZnO QD films. **Table 1** shows the four different nitrile solvents investigated in this work with their melting points. Compared to succinonitrile, trans-3-hexenedinitrile has a longer carbon chain, cyanoacetamide can form hydrogen bonds and both 1,2-dicyanobenzene and 1,3-dicyanobenzene are aromatic molecules which are expected to demonstrate increased crystallinity when solid. The melting points of these solvents range from 74 to 165 °C.

In addition to having a high melting point the solvents need to be electrochemically stable at the potentials used for electrochemical doping. By adding functional groups such as a benzene or an amine group, the electrochemical stability of the solvent might differ greatly. The electrochemical potential window of the four high melting point nitriles has been determined by cyclic voltammetry (CV) on blank Au electrodes with a scan rate of 50 mV s⁻¹, as illustrated in **Figure 2**. Both LiClO₄ and TBAPF₆ were used as supporting electrolyte. We use a, somewhat arbitrary, cutoff current density of 20 μA cm⁻² to determine the cathodic and anodic stability limits. The resulting limits are shown in Table 1. We find that trans-3-hexenedinitrile is most stable both cathodically and anodically (-1.39 and +1.16 V vs Fc/Fc⁺). In Figure 2a the oxidation peaks on the reverse scan between 0 and 0.5 V versus Fc/Fc⁺ are connected to the reduction of the solvent at around -1.5 V versus Fc/Fc⁺. Therefore, the anodic limit is determined from Figure S1 in the Supporting Information, where a smaller cathodic range was scanned so that no solvent reduction occurred. The electrochemical potential window of the other three solvents is considerably narrower. Of these solvents cyanoacetamide and 1,2-dicyanobenzene are more stable at negative potentials (vs Fc/Fc⁺), while 1,3-dicyanobenzene is more stable at positive potentials (vs Fc/Fc⁺). At last, the effect of different electrolyte salts is small, although LiClO₄ seems to yield a somewhat better stability than TBAPF₆.

Table 1. Melting points and electrochemical potential windows for different nitriles. Either LiClO₄ or TBAPF₆ was used as supporting electrolyte. 20 μA cm⁻² was chosen as the cutoff current density for the potential window.

Solvent	Melting point [°C]	Chemical Structure	Cathodic limit, LiClO ₄ [V vs Fc/Fc ⁺]	Anodic limit, LiClO ₄ [V vs Fc/Fc ⁺]	Cathodic limit, TBAPF ₆ [V vs Fc/Fc ⁺]
Trans-3-hexenedinitrile	74–79		-1.39	1.16	-
Cyanoacetamide	119–121		-1.07	0.26	-1.03
1,2-dicyanobenzene	137–139		-0.92	0.44	-0.67
1,3-dicyanobenzene	163–165		-0.29	1.00	-

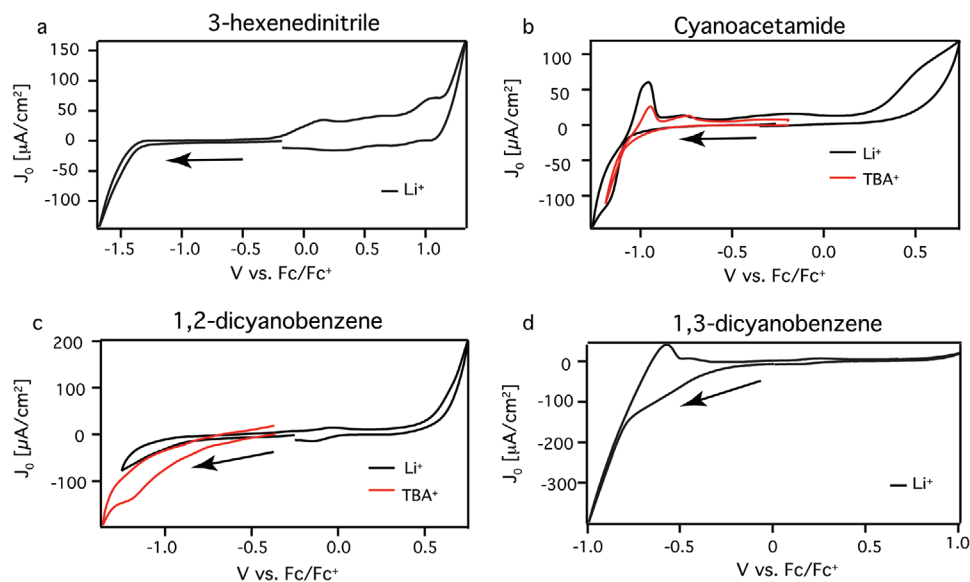


Figure 2. Electrochemical potential window measurements in different electrolyte solvents. The CVs are performed with blank Au electrodes in a) trans-3-hexenedinitrile, b) cyanoacetamide, c) 1,2-dicyanobenzene, d) 1,3-dicyanobenzene. The solvents contain 0.1 M of either LiClO_4 (black trace) or TBAF_6 (red trace) and the scan rate is 50 mV s^{-1} . The scan is started around -0.3 V versus Fc/Fc^+ and is initially scanned in the cathodic direction (indicated by arrows in the Figure).

To see if these solvents are suitable for electrochemical doping, we performed electrochemical measurements with ZnO QD films. This material is selected as it exhibits stable and reversible electron injection, and furthermore allows multiple measurements to be performed on the same sample.^[9a,15] Figure 3 shows CVs and Fermi-level stability measurements for ZnO QD films in 0.1 M LiClO_4 nitrile solutions. The measurements were performed at two different temperatures, above the melting point and at room temperature (20°C).

Figure 3a shows CVs performed in trans-3-hexenedinitrile at both 100°C and RT. In the first case, the CV shows clear charging and discharging of the ZnO QD film similar to CVs on such films using, e.g., acetonitrile at RT.^[8d,9a] However, upon lowering the temperature the current density decreases drastically. A zoom-in of a CV at room temperature in trans-3-hexenedinitrile is shown in Figure S2 in the Supporting Information. It exhibits a minor, but detectable difference in current density on the forward and backward scan. This shows that the movement of electrolyte ions has been decreased immensely, but that some charging/discharging still takes place.

Figure 3b shows CVs in cyanoacetamide at both 140°C and RT. As for trans-3-hexenedinitrile the current decreases drastically by lowering the temperature. However, a zoom-in of the CV at room temperature (Figure S3, Supporting Information) shows no sign of charging/discharging for this solvent. In fact the CV looks very similar to what is measured when the potentiostat is disconnected (Figure S4, Supporting Information). This means that the electrolyte ions are effectively immobilized in the frozen solvent. Figure 3e,f shows the same trend for both 1,2-dicyanobenzene and 1,3-dicyanobenzene. The magnified versions of the CVs at room temperature are in Figures S5 and S6 in the Supporting Information, and again no charging currents are seen.

From the measured current in the CVs at high temperature, it is possible to calculate the charging ratio between injected and extracted electrons by the use of Equation (1)

$$\frac{n_{\text{extr}}}{n_{\text{inj}}} = \frac{\sum(I * dE)}{\sum(I * dE)} \quad (1)$$

where n_{extr} is the number of extracted electrons, n_{inj} is the number of injected electrons, I is the measured current and dE is the potential step. We find that in trans-3-hexenedinitrile 88% of injected electrons are extracted. This number is slightly lower for cyanoacetamide (72%). On the other hand, it drops to 6% and 0% for 1,2-dicyanobenzene and 1,3-dicyanobenzene, respectively. These numbers can be related to the electrochemical (in)stability of the solvents shown in Figure 2. At potentials where electron charging occurs (roughly negative of -0.6 V vs Fc/Fc^+) 1,2-dicyanobenzene and 1,3-dicyanobenzene show non-negligible cathodic currents. This implies that the solvent can react with the electrons injected into the ZnO QDs and explains why they are not extracted.

Figure 3c,d,g,h shows Fermi-level stability measurements for ZnO QD films in the different nitriles: the films are charged when the solvent is liquid, then the counter electrode (CE) is disconnected so that no more charging or discharging is possible via the external circuit. If electrons disappear from the ZnO QD film, the measured potential will decay towards its original open circuit potential before the film was charged. If no electrons leave the QDs, the measured potential is stable. For the measurements at room temperature, the CE was disconnected after room temperature was reached. From these measurements it is clear that the measured potential decays drastically faster at high temperatures than at RT. As shown in Figure 3c, a small drop in potential is seen for trans-3-hexenedinitrile over the course of two hours at RT. This potential decay can be related to the slight charging

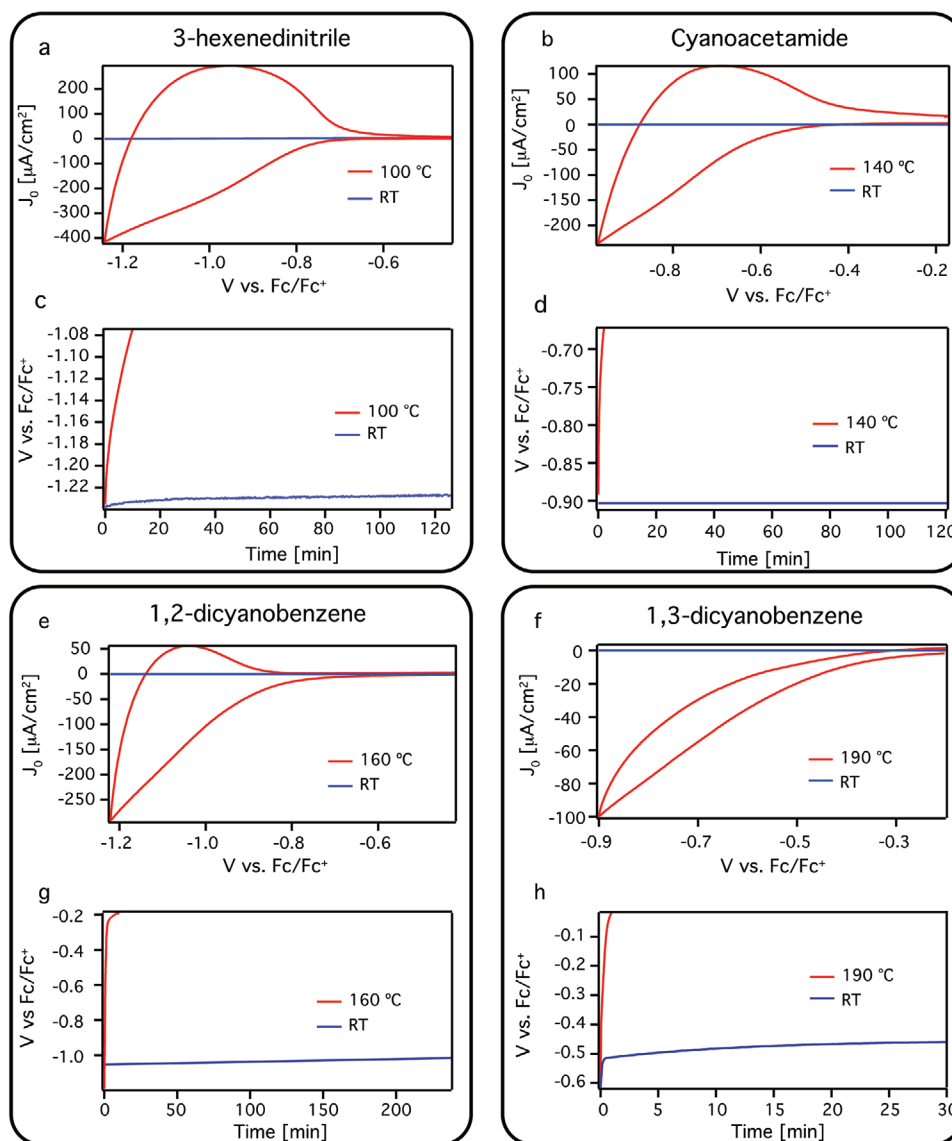


Figure 3. Electrochemical measurements performed with ZnO QD films in different nitrile solvents. CVs are performed with a scan rate of 50 mV s^{-1} performed in a 0.1 M LiClO_4 a) trans-3-hexenedinitrile solution, b) cyanoacetamide solution, e) 1,2-dicyanobenzene solution, and f) 1,3-dicyanobenzene solution. Fermi-level stability measurements performed in a 0.1 M LiClO_4 c) trans-3-hexenedinitrile solution, d) cyanoacetamide solution, g) 1,2-dicyanobenzene solution, h) 1,3-dicyanobenzene solution. The red traces show measurements performed when the solvent is liquid, while the blue traces show measurements performed at room temperature.

and discharging current in the CV at room temperature. This charging current suggests that the solvent is not entirely frozen. We conjecture that this also allows some diffusion of impurities such as molecular oxygen, which can react with the injected electrons and lower the potential. On the other hand, the potential in cyanoacetamide at RT does not decay at all during the two hours shown (Figure 3d). For 1,2-dicyanobenzene a small drop in the potential is seen at RT (Figure 3g) while a much faster drop in potential is seen for 1,3-dicyanobenzene (Figure 3h). As this is in line with the ratio of the extracted and injected electrons in the CVs, this potential decay can be related to the limited cathodic stability of these solvents.

From these experiments it is clear that the solvent stability plays an equally important role as the melting point in

producing stable electrochemically doped films at room temperature. To see this even clearer, **Figure 4** shows a comparison of 6 different nitriles that were used in our previous study and this study.^[9a] The nitriles are: acetonitrile (ACN, mp: $-45 \text{ }^\circ\text{C}$), succinonitrile (SuN, mp: $57 \text{ }^\circ\text{C}$), trans-3-hexenedinitrile (3-HDN, mp: $76 \text{ }^\circ\text{C}$), cyanoacetamide (CAA, mp: $120 \text{ }^\circ\text{C}$), 1,2-dicyanobenzene (1,2-DCB, mp: $138 \text{ }^\circ\text{C}$) and 1,3-dicyanobenzene (1,3-DCB, mp: $164 \text{ }^\circ\text{C}$). In Figure 4 the peak current density at RT and the change in the potential, ΔV , observed in Fermi-level stability measurements over 30 min at RT are shown for the different solvents. The RT current density and drop in Fermi-level generally decrease with increasing melting point. However, we do not observe that the solvents with the highest melting points have the best Fermi-level stability, since the two solvents with the

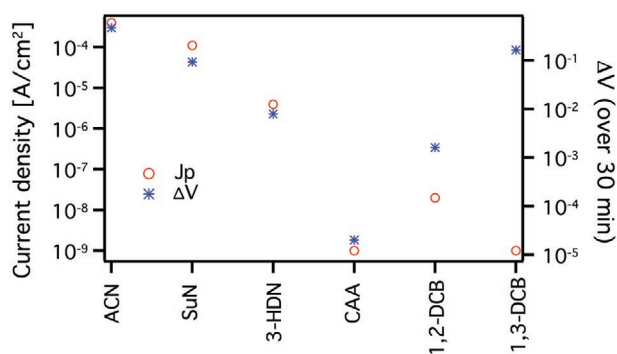


Figure 4. Current peak densities (J_p , red circles) and potential decay over 30 min in Fermi-level stability measurements (ΔV , blue stars) for different nitrile solvents at room temperature. Used solvents are: acetonitrile (ACN, mp: $-45\text{ }^\circ\text{C}$), succinonitrile (SuN, mp: $57\text{ }^\circ\text{C}$), trans-3-hexenedinitrile (3-HDN, mp: $76\text{ }^\circ\text{C}$), cyanoacetamide (CAA, mp: $120\text{ }^\circ\text{C}$), 1,2-dicyanobenzene (1,2-DCB, mp: $138\text{ }^\circ\text{C}$), and 1,3-dicyanobenzene (1,3-DCB, mp: $164\text{ }^\circ\text{C}$). The peak current density for both cyanoacetamide and 1,3-dicyanobenzene is within the noise of the measurements ($\approx 1\text{ nA}$).

highest melting point show (minor) cathodic decomposition at the potentials used. By taking all these results into account we conclude that cyanoacetamide is the most promising solvent for obtaining a stable electrochemically n-doped semiconductor film at room temperature. Therefore, further measurements were performed with cyanoacetamide.

Figure 5a shows CVs performed on ZnO QD films in 0.1 M LiClO_4 cyanoacetamide solution at temperatures between 140 and $0\text{ }^\circ\text{C}$ with a 10 degree interval. **Figure 5b** shows the peak current density as a function of temperature. A decrease of 6 orders of magnitude is observed. We have previously shown

that the charging current is limited by cation diffusion.^[8d] Thus the decreasing current density results from a decreasing diffusion coefficient of the electrolyte cations.

Differential scanning calorimetry measurements indicate that the electrolyte salt causes a melting point reduction of at most $9\text{ }^\circ\text{C}$. For 0.1 M LiClO_4 in cyanoacetamide a recrystallization temperature of $75.6\text{ }^\circ\text{C}$ was measured (Figures S7–S9, Supporting Information). Interestingly, no clear phase transition is seen in **Figure 5b** at $75\text{ }^\circ\text{C}$. This suggests that the crystallization inside the pores of the QD film is hindered and occurs over a wide temperature range. Full crystallization requires temperatures well below the melting point of the pure solvent.

We calculate the diffusion coefficient from the peak current density with the Randles-Sevcik equation

$$j_p = 0.4463nFAC \left(\frac{nFvD}{RT} \right)^{0.5} \quad (2)$$

where j_p is the peak current density, n is the number of electrons, F is the Faradaic current, A is the electrode area, C^* is the concentration of the electrolyte, v is the scan rate, D is the diffusion coefficient, R is the gas constant and T is the temperature. The diffusion coefficient is plotted on the right axis in **Figure 5b**. Values below $80\text{ }^\circ\text{C}$ are an approximation of the diffusion coefficient as no clear charging maxima are seen in these CVs (**Figure S10**, Supporting Information). Instead we used the lowest measured current (at around -1 V vs Fc/Fc^+). At $140\text{ }^\circ\text{C}$ the diffusion coefficient of Li^+ in cyanoacetamide is $\approx 10^{-9}\text{ cm}^2\text{ s}^{-1}$, whereas at RT, it is 12 orders of magnitude lower, or around $10^{-21}\text{ cm}^2\text{ s}^{-1}$. Considering the latter value, we can estimate that it would take a Li^+ ion $\approx 10^{13}\text{ s}$ ($>300\,000$ years) to diffuse out of a $1\text{ }\mu\text{m}$ thick ZnO QD film.

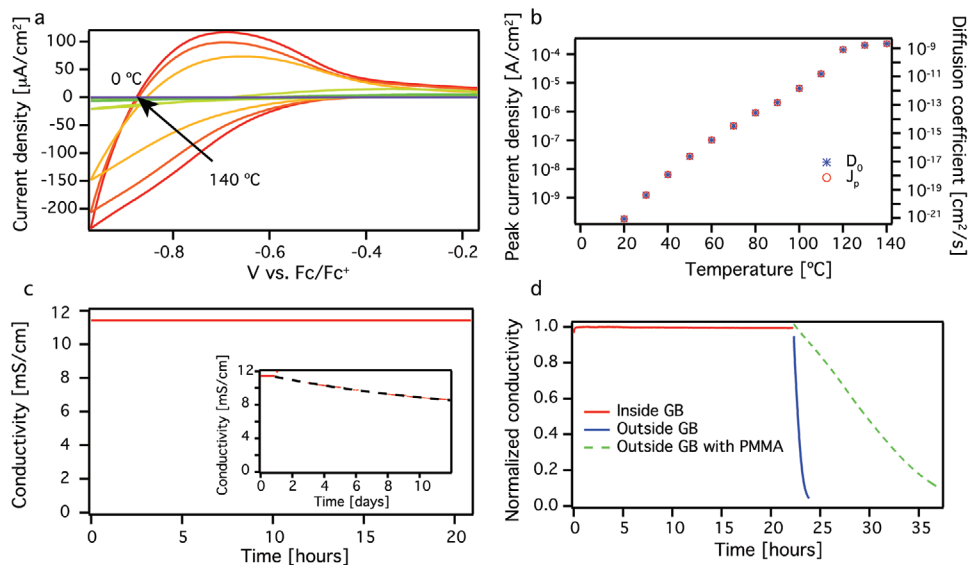


Figure 5. Electrochemical measurements for a ZnO QD film in 0.1 M LiClO_4 cyanoacetamide solution. a) CVs performed between 140 and $0\text{ }^\circ\text{C}$ with 10 degrees interval. The scan rate is 50 mV s^{-1} . b) The peak current density obtained from the CVs (red circles) and the calculated diffusion coefficient (blue stars). c) Source–drain electronic conductivity measurements for the ZnO QD film after it has been taken out of the cyanoacetamide solution. The measurement is carried out at room temperature, so the solution has solidified. The panel includes an inset that shows the measurements on a longer time scale, the black trace is a guide to the eyes for the decay of the conductivity. d) Electronic conductivity measurements performed both inside (red trace) and outside (blue trace) of the glovebox on a ZnO QD film measured outside of the electrochemical cell. The panel also shows conductivity measurements outside of the glovebox where a PMMA layer was added on top of the solid cyanoacetamide (green trace).

So far, in all the measurements the ZnO QD film has been submerged in the electrolyte solvent. That is, the film was inside a metal cell with a block of frozen solvent around it. Clearly, this configuration is not suitable for use in semiconductor devices. Therefore we also performed experiments where the film is removed from the electrolyte solution after electrochemical doping. The film is charged at 140 °C when the solvent is liquid, the potentiostat is disconnected and the film is quickly removed from the cell, causing the temperature to drop and the cyanoacetamide to solidify. Since in this case we cannot measure the potential versus a reference electrode we now use source–drain electronic conductivity measurements to test the doping stability, employing a home-built interdigitated electrode (IDE) (Figure 5c, see an image of the film in Figure S11 in the Supporting Information). The advantage of such conductivity measurements is that they do not require additional electrodes and can be performed on the doped film directly. Since the conductivity σ is linearly related to the charge density n via $\sigma = ne\mu$, where μ is the electron mobility, the charge stability can be probed sensitively by measuring the conductivity. In comparison, the potential in Fermi-level stability measurements decays logarithmically with the charge carrier density, as expressed by the Nernst law.

Figure 5c shows that for the first 20 hours the conductivity does not decrease at all (see a magnified version in Figure S12 in the Supporting Information), in line with the enhanced Fermi-level stability shown in Figure 3d. However, on much longer time scales the conductivity starts to gradually decrease (see inset in Figure 5c): after 10 days around 20% of injected charge has left the ZnO QD film (see a normalized graph in Figure S13 in the Supporting Information).

Since the conductivity did not decrease in the beginning of the measurement, we speculate that this gradual decrease on longer time scales might be due to molecular oxygen. We have shown in a previous study the great impact of impurities, such as oxygen, on the doping stability of ZnO QD films.^[10b] Even the controlled atmosphere of a nitrogen filled glovebox contains impurities, most notably oxygen, in very low concentrations (the oxygen level of the glovebox used is typically <1 ppm). Therefore, if the solid cyanoacetamide film does not protect the ZnO QD film against diffusion of oxygen, given long enough time oxygen molecules will reach and oxidize the QDs. The diffusion of oxygen in cyanoacetamide is likely influenced by the fact that cyanoacetamide does not form a smooth consistent layer when it solidifies. Molecular oxygen has a standard reduction potential of ≈ -1.2 V versus Fc/Fc⁺.^[16] However, this reaction is often irreversible, meaning that even electrons at less negative potentials (such as the electrons in the ZnO QDs which have a potential between -0.6 and -1.2 V versus Fc/Fc⁺ in this experiment, set by the potential used during charging), will react with oxygen given long enough time.

In order to see if this is the case, we performed source–drain electronic conductivity measurements on a ZnO QD film both inside and outside of the nitrogen filled glove box (Figure 5d). Inside the glovebox the conductivity is stable in the first 20 hours. When the film is brought outside of the glovebox, the conductivity drops to intrinsic values in less than two hours. This shows that even if the cyanoacetamide solvent is frozen and immobilizes the electrolyte cations, it does not fully protect the film against oxygen.

One way of protecting the ZnO QD film against oxygen is to apply a protective layer on top of the cyanoacetamide solid layer. Figure 5d shows a measurement for a ZnO QD film in 0.1 M LiClO₄ cyanoacetamide solution with a poly(methyl methacrylate) (PMMA) layer on top of it, measured outside of the glove box. In this case it takes over 15 hours for the electronic conductivity to drop, compared to two hours when no PMMA is used. Since the protection of the film with PMMA has not at all been optimized, this gives hope that much higher stabilities could be reached. One notable interesting approach would be to use a thin alumina coating, which can for instance be deposited using ambient temperature Atomic Layer Deposition.^[17]

Since cyanoacetamide as a frozen electrolyte solvent works well to increase the stability of electrochemically doped ZnO QD films, it is of interest to see if this method can also be applied to other semiconducting materials. **Figure 6** shows results for both films of PbS QDs and the conductive polymer P3DT. Films of PbS QDs can be n-doped,^[18] while films of P3DT are easily p-doped electrochemically.^[9a,19]

Figure 6a shows CVs for a PbS QD film in cyanoacetamide at 140 °C and at room temperature. At 140 °C there is a large current density, corresponding to charging and discharging of the PbS QDs with electrons. The clear separation between the reduction peak around -1.0 V and the oxidation peak around -0.8 V versus Fc/Fc⁺ is only observed when LiClO₄ is used as an electrolyte, but not when TBAPF₆ is used (see Figure S14 in the Supporting Information) and is probably an indication that Li⁺ intercalation takes place.^[20] As expected, at room temperature the current density in the CV has decreased drastically (a magnified version is shown in Figure S15 in the Supporting Information), as a result of the freezing of the solvent.

A similar trend is seen for P3DT in Figure 6b. At RT only negligible charging/discharging is observed (see Figure S16 in the Supporting Information for a zoom in). At 140 °C the CV for P3DT shows clear hole injection at positive potentials, although no negative current is obtained in the reverse scan, indicating the holes are not extracted. If we look at Table 1 the anodic limit for cyanoacetamide is 0.262 V versus Fc/Fc⁺ and we are scanning to 0.3 V versus Fc/Fc⁺. Therefore, we assume that cyanoacetamide partially oxidizes at this positive potential by reacting with the holes in the P3DT. 1,3-dicyanobenzene might be a better choice as electrolyte solvent for P3DT. On the other hand, it simplifies the doping process of semiconductor films if both p and n-type doping can be performed in the same electrolyte solvent.

For both PbS QDs and P3DT we performed source–drain electronic conductivity measurements in cyanoacetamide at RT after electrochemical doping at 140 °C. The conductivity is plotted for the PbS QD film in Figure 6c and for the P3DT film in Figure 6d. Figure 6c, shows that for the PbS QD film, the conductivity is constant for over 5 days (see also Figure S17 in the Supporting Information), before it starts to gradually decrease. After 40 days the conductivity has decreased by 9.6%. If the film is taken out of the glovebox it is seen that the rest of the charge leaves the PbS QD film within 2 hours (inset in Figure 6c). This shows that oxidation by molecular oxygen is responsible for the drop in electron density. As for the ZnO QD film an additional oxygen blocking layer is needed.

Figure 6d shows the conductivity for a P3DT film. Interestingly, after 76 days of measurements the conductivity has only

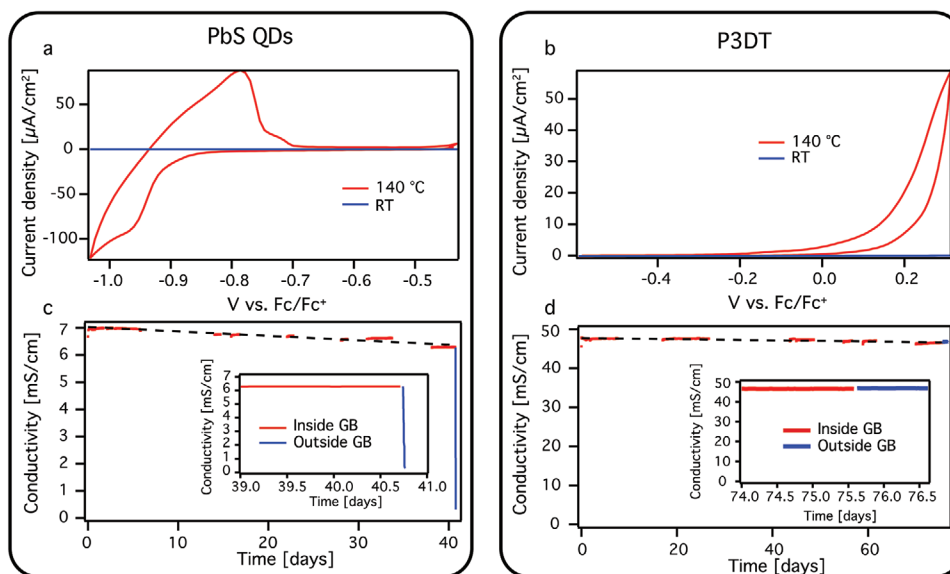


Figure 6. Doping other semiconducting materials in 0.1 M LiClO₄ cyanoacetamide. a) CVs for a PbS QD with TBAI as cross-linking ligands film at 140 °C (red trace) and RT (blue trace), the scan rate is 50 mV s⁻¹. b) CVs for a P3DT film at 140 °C (red trace) and RT (blue trace), the scan rate is 50 mV s⁻¹. c) Conductivity for a PbS QD film with TBAI as cross-linking ligands measured outside the electrochemical cell at room temperature both before and after it is taken out of the nitrogen filled glovebox. The black trace is a guide to the eye for the decay of the conductivity. The panel includes an inset which shows the conductivity in approximately the last two days of measurements. d) Conductivity for a P3DT film measured outside of the electrochemical cell at room temperature, both inside and outside of the glovebox. The panel includes an inset which shows the conductivity in approximately the last two days of measurements. The black trace is a guide to the eye for the decay of the conductivity. When the film is brought out of the cell, cyanoacetamide solidifies on top of the film.

dropped by 2% (see Supporting Information, Figure S18 in the Supporting Information for a magnification). Furthermore, when the film is taken out of the glovebox, the conductivity is not affected at all (inset in Figure 6d). This shows, that even if the doping takes place at the edge of the anodic limit for cyanoacetamide, the frozen solvent is still stable enough to maintain p-doping of the P3DT film. Additionally, the conductivity doesn't decrease gradually over time as for ZnO and PbS QD films. The main difference between these materials is that PbS and ZnO QD films are doped n-type while the P3DT film is doped p-type. Oxidation by molecular oxygen will not occur at the Fermi-level of the p-doped P3DT, and would not decrease the hole density even if it did. Rather, the risk is in reduction by other impurities such as water. As the conductivity does not decrease when the film is taken out of the glovebox, it shows that cyanoacetamide is a great diffusion barrier against impurities that oxidize at these potentials (such as water).

These measurements show that it is possible to obtain stable electrochemically doped semiconductor films made of both QDs (PbS and ZnO) and conductive polymers (P3DT) by the use of cyanoacetamide at room temperature. Unfortunately, the cyanoacetamide doesn't protect the films against oxygen in the case for n-type doping, while the p-type doping is stable. Therefore, it is important to find solvents which recrystallize in such a way that they protect the doped films against oxygen. Additionally, the electrochemical potential window of cyanoacetamide is too limited for doping of various semiconductors. For example, potentials of ≈ -1.7 V versus Fc/Fc⁺ are needed to n-dope CdSe QDs, and many organic semiconductors need more positive potentials for p-doping compared to P3DT.^[30,50] At last, this new solvent needs a melting point in the range of

100–200 °C to ensure stable doping at room temperature and that the films survive. If a solvent will fulfill these three requirements, it would be ideal for use to gain stable electrochemical doping at room temperature. To demonstrate that RT frozen solvents can be used to generate semiconductor devices wherein the doping is controlled electrochemically we have used this approach to form pn junction diodes. We have chosen PbS QD films with 1,2-ethanedithiols (EDT) as cross linking ligands to make such a diode, as the QDs can be doped both n and p-type in the electrochemical stability window of cyanoacetamide (Figure S19, Supporting Information). **Figure 7a** shows a schematic of how the home-built interdigitated gold electrode (IDE) can be used to make a pn-junction diode (a photograph of the IDE is shown in Figure S20 in the Supporting Information). The PbS QD film is deposited on the IDE. If a voltage larger than the bandgap of the PbS QDs is applied over the two interdigitated electrodes, this results in n-doping on one electrode and p-doping on the other. Hence, a dynamic pn junction is formed, similar to what happens in luminescent electrochemical cells.^[17] However, by removing the film from the hot cyanoacetamide solution and allowing the solvent to solidify, the dynamic pn junction transforms into a static pn junction and a stable diode should form.

Figure 7b shows two IV measurement (see Experimental Methods) for PbS QD films performed in 0.1 M LiClO₄ cyanoacetamide at room temperature. In the first measurement the sample is uncharged (no bias is applied between the two working electrodes), and a symmetric curve is seen, as expected. However, by applying a 1.4V bias (more than the 1 eV bandgap of the PbS QDs) between the two interdigitated electrodes a strongly asymmetric IV curve is obtained. This diode-like curve demonstrates that the pn junction is indeed

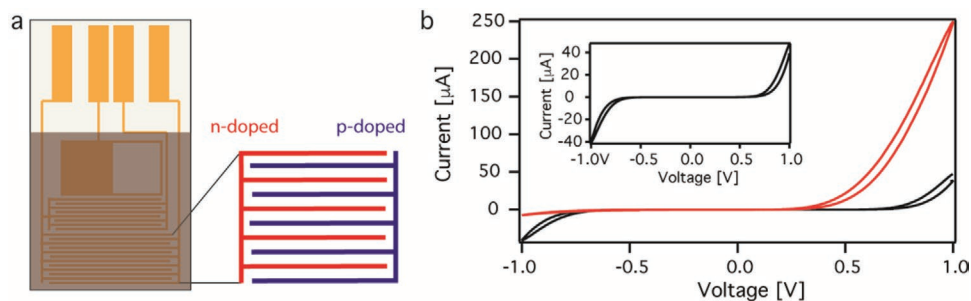


Figure 7. PbS QD films diode measurements. a) A schematic of a home-built interdigitated electrode (IDE) containing a PbS QD film. The interdigitated electrodes are used for the formation of a pn-junction diode by doping a part of the sample n-type with one working electrode and the rest of the sample p-type with second working electrode. b) Diode measurements for a PbS QD film with EDT as a cross-linking ligand in 0.1 M LiClO₄ cyanoacetamide at room temperature. The panel includes an uncharged film (0 V bias applied over the film, black trace) and a measurement where 1.4 V bias is applied between the two working electrodes (red trace). A magnification of the uncharged measurements is an inset.

formed. The application of a large bias does not destroy the pn junction since ions can no longer move in the frozen solvent. The obtained ratio of the current at forward bias compared to reversed bias is between 10 and 40 for multiple samples. This shows that a diode is formed, albeit there is room for improvement.

3. Conclusion

In summary, we have investigated different nitriles with high melting points as electrochemical solvents, to obtain stable electrochemically doped semiconductor films at room temperature. We showed that the stability of n-doping in ZnO QD films is related to both the electrochemical stability windows and the melting point of the solvents. In the end both the melting point and the solvent stability determine the suitability of the solvent for a stable doping by room temperature freezing. The best results for ZnO QD films were obtained with cyanoacetamide, as the electrolyte ions are completely immobilized at room temperature. Conductivity measurements of ZnO QD films charged in cyanoacetamide showed that the doping density is completely stable over 20 hours at room temperature. At longer timescales the conductivity starts to gradually decrease, and after 10 days around 20% of the injected electrons have left the ZnO QD film. This decrease is likely due to oxidation by molecular oxygen that penetrates the frozen cyanoacetamide. At last, we performed electrochemical measurements in cyanoacetamide for two other semiconductors, PbS QDs and the conductive polymer P3DT. The n-doped PbS QD film was stable for over 5 days, but after 40 days, around 10% of the injected electrons had disappeared. On the other hand, the p-doped P3DT film was stable over the full 76 days of the measurement (conductivity decreased by only 2%). Finally we demonstrate a pn-junction diode made of a PbS QD film wherein the p and n regions were formed electrochemically in cyanoacetamide at elevated temperature and were stabilized by cooling to room temperature. These results show that electrochemical doping combined with room temperature freezing of the solvent is a promising method to prepare permanently doped semiconductor thin films, composed of for instance colloidal QDs or organic semiconductors.

4. Experimental Section

Materials: Zinc acetate dihydrate (Zn(CH₃COO)₂·2H₂O reagent grade), potassium hydroxide (KOH pellets), cadmium oxide (CdO, 99.999%), oleic acid (OA, 90%), 1-octadecene (ODE, 90%), sulfur powder (S, 99.99%), oleylamine (OLA, 70%), lead chloride (PbCl₂, 99.999%), poly(3-decylthiophene-2,5-diyl) (P3DT), indium-doped tin oxide substrates (ITO, PGO Germany), lithium perchlorate (LiClO₄, 99.99%), tetrabutylammonium hexafluorophosphate (TBAPF₆, 98%), tetrabutylammonium iodide (TBAI, ≥99%), 1,2-ethanedithiol (EDT, ≥98%), poly(methyl methacrylate) (PMMA), ferrocene (Fc, 98%), trans-3-hexendinitrile (97%), cyanoacetamide (99%), 1,2-dicyanobenzene (98%), 1,3-dicyanobenzene (98%), anhydrous solvents (acetonitrile, 99.99%, methanol, 99.8%, ethanol (maximum 0.01% H₂O), hexane, 95%, chloroform, 99+%) were all purchased from Sigma-Aldrich unless stated otherwise. Acetonitrile was dried before use in an Innovative Technology PureSolv Micro column. All other chemicals were used as received.

ZnO Synthesis: ZnO synthesis was performed in air as previously described.^[8d] Zinc acetate dihydrate (3.425 mmol) were dissolved in ethanol (50 mL) at 60 °C in an Erlenmeyer flask. In a separate vial, KOH (6.25 mmol) was dissolved in methanol (5 mL), and added dropwise to the stirred Zinc mixture. After a wait of 1 to 2 min the ZnO QDs were removed from the heat source and washed by addition of toluene. The flocculates were isolated by centrifugation at 2000 rpm for 1 min and redissolved in ethanol. The mixture was kept in a freezer at -20 °C to avoid further growth.

PbS Synthesis: PbS QDs were synthesized following the procedure of Zhang et. al.^[22] where CdS QDs were initially synthesized and PbS QDs were formed by Pb for Cd cation exchange.

CdS QDs were synthesized by initially heating a mixture of CdO (1 mmol, 0.128 g), OA (3 mmol, 0.942 g) and ODE (15 g) for 20 min at 260 °C, then the temperature was set to 250 °C. The sulfur precursor was made by dissolving S powder in ODE (0.5 M) at 130 °C. 1 mL of the sulfur precursor was injected into the Cd precursor at 250 °C, the solution was maintained at 240 °C. After about 13 min additional sulfur precursor was added to the solution drop wise until the desired size was reached. The CdS QD solution was washed twice with hexane and ethanol and centrifuged at 7500 rpm for 5 min. The CdS QDs were redissolved in ODE.

For the PbS QDs, PbCl₂ (1.5 mmol) was dissolved in OLA (5 mL) at 140 °C for 30 min until a white turbid solution was formed. The solution was heated to 190 °C and 1 mL of the CdS QDs was injected swiftly. The solution was quenched with a water bath 20 s later. At 70 °C 5 mL of hexane were added and at 40 °C 4 mL of OA were added. The solution was washed 3 times with hexane and ethanol and centrifuged at 7500 rpm for 5 min. The PbS QDs were redissolved in hexane.

Film Preparation: All films were deposited on two different working electrodes (WE). The former one was an ITO electrode while the second one was a home-built interdigitated gold electrode (IDE) (see Figure S20

in the Supporting Information). The ZnO quantum dot films were drop-casted on top of the substrate in air and annealed at 60 °C for an hour.

The PbS quantum dot films were made by dip-coating, either by using TBAI or 1,2-ethanedithiol (EDT) as cross-linking ligands.

Film Preparation—TBAI: Initially the substrate was dipped in the quantum dot solution, followed by dipping the substrate in methanol containing TBAI (11 mg mL⁻¹). The substrate was kept in the solution for around 30 s before being washed in a methanol solution for about 10 s.

Film Preparation—EDT: Initially the substrate was dipped in the quantum dot solution, followed by dipping the substrate in 1 × 10⁻³ M EDT in acetonitrile. Thereafter, the substrate was washed in an acetonitrile solution for about 10 s.

For the P3DT films, 10 mg mL⁻¹ of P3DT were dissolved in 1,2-dichlorobenzene. The solution was spin coated on the substrate for 60 s at 3000 RPM, with a ramp of 1000 RPM s⁻¹.

When PMMA was used as a protective layer, the PMMA solution (5 w% in chloroform) was drop casted on top of the film. This process was repeated several times.

Electrochemical Measurements: All electrochemical measurements were performed in a nitrogen filled glovebox (moisture < 0.05 ppm and O₂ level < 0.1 ppm) unless stated otherwise. The measurements were performed either with an Autolab PGSTAT128N or Autolab PGSTAT204 potentiostat in a three electrode electrochemical cell. The working electrode (WE) was either ITO or a gold IDE, the counter electrode (CE) was a platinum sheet and the reference electrode (RE) was a Ag pseudoreference electrode. The reference electrode was calibrated with the ferrocene/ferrocenium (Fc/Fc⁺) couple before every measurements, and all potentials were given versus the Fc/Fc⁺ couple.

Source–Drain Electronic Conductivity Measurements: The source–drain electronic conductivity measurements were performed as previously described with the homemade IDE.^[10b] Initially, the semiconductor film was charged by the use of a potentiostat. After a desired doping density was reached, the sample was disconnected from the potentiostat and the source–drain electronic conductance was measured with a Keithly 2400 source meter. After the potentiostat was disconnected, charges could no longer be injected into the semiconductor. The used source–drain potential was 10 mV.

From the measured conductance, the conductivity, σ , can be calculated with Equation (3)

$$\sigma = \frac{G \times w}{l \times h} \quad (3)$$

where G is the conductance, w is the source–drain width, l is the gap length and h is the height of the sample.

For calculation of the conductivity for ZnO QD films, a common thickness of 1 μm is used.^[10b]

For calculation of the conductivity for both PbS QD films and P3DT films, thickness measurements proved complicated due to the solid cyanoacetamide layer on top of the film. Therefore, the thickness of a PbS QD film and a P3DT film made in the same way were used. By using Dektak profilometer, the thickness for the PbS QD film was measured as approximately 90 nm, while it was approximately 30 nm for the P3DT film.

Fermi-Level Stability Measurements: Fermi-level stability measurements were performed as previously described.^[9a,10b] The sample was charged with a potentiostat, and when a desired doping density was reached and the system had reached an equilibrium, the CE was disconnected from the cell. This means that electrons could no longer be injected or extracted from the semiconductor film, while the potential of the WE versus the RE was monitored. The measured potential was connected to the Fermi-level of the film. If injected charges left the film, the Fermi-level decayed into the band gap of the semiconductor. This means that the potential would decay to its original value (the open circuit potential) before charge injection took place.

Diode Measurements: pn-junction diodes were made from PbS QD films on inter-digitated gold electrodes (IDE). The PbS QD film was deposited on the IDE as explained above and the film was placed in liquid cyanoacetamide (around 140 °C). The diode was made by applying

a potential bias over two contacts of the interdigitated electrodes with a Keithly 2400 source meter, then the film was taken out of the warm cyanoacetamide solution and the solvent solidifies. When the system had reached room temperature (the cyanoacetamide had solidified), the IDE was disconnected from the Keithly 2400 source meter. The IV curves were measured with an Autolab PGSTAT128N potentiostat where the CE and RE were connected to one gold electrode, while the other gold electrode was connected to the WE of the potentiostat.

Supporting Information

Supporting Information is available from the Wiley Online Library or from the author.

Acknowledgements

The authors want to acknowledge Ben Norder for measuring their solvents with DSC. The authors also want to acknowledge Rienk Elkema for the discussion about organic chemistry. A.J.H. acknowledges support from the European Research Council Horizon 2020 ERC Grant Agreement No. 678004 (Doping on Demand).

Conflict of Interest

The authors declare no conflict of interest.

Keywords

charge stability, electrochemical doping, electrolyte solvents, porous semiconductors, quantum dots

Received: June 5, 2020

Revised: August 3, 2020

Published online:

- [1] D. V. Talapin, J.-S. Lee, M. V. Kovalenko, E. V. Shevchenko, *Chem. Rev.* **2010**, *110*, 389.
- [2] a) R. E. Bailey, S. Nie, *J. Am. Chem. Soc.* **2003**, *125*, 7100; b) A. I. Ekimov, A. I. L. Efros, A. A. Onushchenko, *Solid State Commun.* **1985**, *56*, 921; c) A. I. Ekimov, F. Hache, M. C. Schanne-Klein, D. Ricard, C. Flytzanis, I. A. Kudryavtsev, T. V. Yazeva, A. V. Rodina, A. L. Efros, *J. Opt. Soc. Am. B* **1993**, *10*, 100; d) B. Geffroy, P. le Roy, C. Prat, *Polym. Int.* **2006**, *55*, 572; e) V. Coropceanu, J. R. Cornil, D. A. D. S. Filho, Y. Olivier, R. Silbey, J.-L. Bredas, *Chem. Rev.* **2007**, *107*, 926; f) F. Würthner, *Pure Appl. Chem.* **2006**, *78*, 2341.
- [3] a) S. C. Boehme, J. M. Azpiroz, Y. V. Aulin, F. C. Grozema, D. Vanmaekelbergh, L. D. Siebbeles, I. Infante, A. J. Houtepen, *Nano Lett.* **2015**, *15*, 3056; b) X. Lan, O. Voznyy, F. P. Garcia de Arquer, M. Liu, J. Xu, A. H. Proppe, G. Walters, F. Fan, H. Tan, M. Liu, Z. Yang, S. Hoogland, E. H. Sargent, *Nano Lett.* **2016**, *16*, 4630; c) H. Wang, Y. Wang, B. He, W. Li, M. Sulaman, J. Xu, S. Yang, Y. Tang, B. Zou, *ACS Appl. Mater. Interfaces* **2016**, *8*, 18526; d) Y. Shirasaki, G. J. Supran, M. G. Bawendi, V. Bulović, *Nat. Photonics* **2012**, *7*, 13; e) F. Fan, O. Voznyy, R. P. Sabatini, K. T. Bicanic, M. M. Adachi, J. R. McBride, K. R. Reid, Y. S. Park, X. Li, A. Jain, R. Quintero-Bermudez, M. Saravanapavanantham, M. Liu, M. Korkusinski, P. Hawrylak, V. I. Klimov, S. J. Rosenthal, S. Hoogland, E. H. Sargent, *Nature* **2017**, *544*, 75; f) J. Gao, G. Yu,

- A. J. Heeger, *Appl. Phys. Lett.* **1997**, *71*, 1293; g) G. Qian, Y. Lin, G. Wantz, A. R. Davis, K. R. Carter, J. J. Watkins, *Adv. Funct. Mater.* **2014**, *24*, 4484; h) A. R. Murphy, J. M. J. Frechet, *Chem. Rev.* **2007**, *107*, 1066; i) Q. Pei, G. Yu, C. Zhang, Y. Yang, A. J. Heeger, *Science* **1995**, *269*, 1086; j) P. Matyba, K. Maturova, M. Kemerink, N. D. Robinson, L. Edman, *Nat. Mater.* **2009**, *8*, 672; k) J. D. Servaites, M. A. Ratner, T. J. Marks, *Energy Environ. Sci.* **2011**, *4*, 4410.
- [4] D. J. Norris, A. L. Efros, S. C. Erwin, *Science* **2008**, *319*, 1776.
- [5] a) A. M. Schimpf, C. E. Gunthardt, J. D. Rinehart, J. M. Mayer, D. R. Gamelin, *J. Am. Chem. Soc.* **2013**, *135*, 16569; b) J. D. Rinehart, A. M. Schimpf, A. L. Weaver, A. W. Cohn, D. R. Gamelin, *J. Am. Chem. Soc.* **2013**, *135*, 18782.
- [6] R. B. Fair, *Impurity Doping Processes in Silicon*, North-Holland Publishing Company, New York **1981**.
- [7] a) A. M. Schimpf, K. E. Knowles, G. M. Carroll, D. R. Gamelin, *Acc. Chem. Res.* **2015**, *48*, 1929; b) M. Shim, C. Wang, D. J. Norris, P. Guyot-Sionnest, *MRS Bull.* **2001**, *26*, 1005; c) I. Salzmann, G. Heimel, M. Oehzelt, S. Winkler, N. Koch, *Acc. Chem. Res.* **2016**, *49*, 370.
- [8] a) P. Guyot-Sionnest, *Microchim. Acta* **2008**, *160*, 309; b) D. Vanmaekelbergh, A. J. Houtepen, J. J. Kelly, *Electrochim. Acta* **2007**, *53*, 1140; c) S. C. Boehme, H. Wang, L. D. A. Siebbeles, D. Vanmaekelbergh, A. J. Houtepen, *ACS Nano* **2013**, *7*, 2500; d) S. Gudjonsdottir, W. van der Stam, N. Kirkwood, W. H. Evers, A. J. Houtepen, *J. Am. Chem. Soc.* **2018**, *140*, 6582.
- [9] a) S. Gudjonsdottir, W. v. d. Stam, C. Koopman, B. Kwakkenbos, W. H. Evers, A. J. Houtepen, *ACS Appl. Nano Mater.* **2019**, *2*, 4900; b) Q. Pei, Y. Yang, G. Yu, C. Zhang, A. J. Heeger, *J. Am. Chem. Soc.* **1996**, *118*, 3922.
- [10] a) I. du Fossé, S. ten Brinck, I. Infante, A. J. Houtepen, *Chem. Mater.* **2019**, *31*, 4575; b) S. Gudjonsdottir, C. Koopman, A. J. Houtepen, *J. Chem. Phys.* **2019**, *151*, 144708.
- [11] a) A. J. Houtepen, Ph.D., Utrecht University, Utrecht, Netherlands **2007**; b) A. J. Houtepen, D. Kockmann, D. Vanmaekelbergh, *Nano Lett.* **2008**, *8*, 3516; c) D. Yu, C. Wang, B. L. Wehrenberg, P. Guyot-Sionnest, *Phys. Rev. Lett.* **2004**, *92*, 216802.
- [12] J. Gao, Y. Li, G. Yu, A. J. Heeger, *J. Appl. Phys.* **1999**, *86*, 4594.
- [13] a) G. Wantz, B. Gautier, F. Dumur, T. N. T. Phan, D. Gigmes, L. Hirsch, J. Gao, *Org. Electron.* **2012**, *13*, 1859; b) C. V. Hoven, H. Wang, M. Elbing, L. Garner, D. Winkelhaus, G. C. Bazan, *Nat. Mater.* **2010**, *9*, 249; c) S. Tang, K. Irgum, L. Edman, *Org. Electron.* **2010**, *11*, 1079.
- [14] a) S. P. Rao, S. Sunkada, *Resonance* **2007**, *12*, 43; b) E. Stauffer, J. A. Dolan, R. Newman, in *Fire Debris Analysis*, Elsevier, Amsterdam **2008**, p. 672.
- [15] M. Shim, P. Guyot-Sionnest, *Nature* **2000**, *407*, 981.
- [16] A. J. Bard, L. R. Faulkner, *Electrochemical Methods Fundamentals and Applications*, John Wiley & Sons, INC., New York **2001**.
- [17] D. Valdesueiro, M. K. Prabhu, C. Guerra-Nunez, C. S. S. Sandeep, S. Kinge, L. D. A. Siebbeles, L. C. P. M. de Smet, G. M. H. Meesters, M. T. Kreutzer, A. J. Houtepen, J. R. van Ommen, *J. Phys. Chem. C* **2016**, *120*, 4266.
- [18] W. K. Koh, A. Y. Kuposov, J. T. Stewart, B. N. Pal, I. Robel, J. M. Pietryga, V. I. Klimov, *Sci. Rep.* **2013**, *3*, 2004.
- [19] M. L. Braunger, A. Barros, M. Ferreira, C. A. Olivati, *Electrochim. Acta* **2015**, *165*, 1.
- [20] V. Augustyn, J. Come, M. A. Lowe, J. W. Kim, P. L. Taberna, S. H. Tolbert, H. D. Abruna, P. Simon, B. Dunn, *Nat. Mater.* **2013**, *12*, 518.
- [21] B. Dandrade, S. Datta, S. Forrest, P. Djurovich, E. Polikarpov, M. Thompson, *Org. Electron.* **2005**, *6*, 11.
- [22] J. Zhang, B. D. Chernomordik, R. W. Crisp, D. M. Kroupa, J. M. Luther, E. M. Miller, J. Gao, M. C. Beard, *ACS Nano* **2015**, *9*, 7151.